JACS
JOURNAL OF THE AMERICAN CHEMICAL SOCIETY
pubs.acs.org/JACS
Communication

2D Hybrid Perovskites Employing an Organic Cation Paired with a Neutral Molecule

Amin Morteza Najarian, Maral Vafaie, Randy Sabatini, Sasa Wang, Peng Li, Shihong Xu, Makhsud I. Saidaminov, Sjoerd Hoogland, and Edward H. Sargent*

Cite This: *J. Am. Chem. Soc.* 2023, 145, 27242−27247
Read Online

ABSTRACT: Two-dimensional (2D) hybrid perovskites harness the chemical and structural versatility of organic compounds. Here, we explore 2D perovskites that incorporate both a first organic component, a primary ammonium cation, and a second neutral organic module. Through the experimental examination of 42 organic pairs with a range of functional groups and organic backbones, we identify five crystallization scenarios that occur upon mixing. Only one leads to the cointercalation of the organic modules with distinct and extended interlayer spacing, which is observed with the aid of X-ray diffraction (XRD) pattern analysis combined with cross-sectional transmission electron microscopy (TEM) and elemental analysis. We present a picture in which complementary pairs, capable of forming intermolecular bonds, cocrystallize with multiple structural arrangements. These arrangements are a function of the ratio of organic content, annealing temperature, and substrate surface characteristics. We highlight how noncovalent bonds, particularly hydrogen and halogen bonding, enable the influence over the organic sublattice in hybrid halide perovskites.

2D hybrid organic−inorganic perovskites (HOIPs) can be envisioned as a series of stacked quantum wells. The inorganic framework forms the wells, while the organic spacers act as barriers.[1−6] This structure allows for a high degree of quantum and dipole confinement, which leads to a substantial exciton binding energy that proves valuable for light-emitting applications.[5,7−12] With their extensive structural and chemical variability, organic cations enable a wide design space for the structure and function in 2D HOIPs. The engineering of organic moieties in noncentrosymmetric perovskite structures has led to spin-splitting,[13] second harmonic generation,[14,15] circular dichroism,[16,17] ferroelectricity,[18−20] and chirality.[15,16,21−23]

2D perovskites, which combine the benefits of both inorganic (rigid crystal backbone) and organic (solution processability) materials, have made significant strides in electro-optic (EO) modulation. However, most 2D hybrid perovskites rely on a limited set of organic substructures.[24,25] Assuming a noncentrosymmetric crystal, the total polarization primarily arises from (i) the ordering of organic dipoles and (ii) the distortion in the inorganic octahedral units. The first source often leads to the self-cancellation of a significant proportion of the organic's molecular dipoles because of oppositely oriented organic bilayers (see Figure 1A,B).

Here, we posit that perovskite structures employing a first organic and a distinct second organic could provide added flexibility in the crystal design (Figure 1C,D). By synthesizing bimolecular structures, we report the possibility of incorporating secondary molecules with high polarizability into organic sublattices. The present study offers thoughts on effective interactions between organic modules and contributing factors in determining the dominant crystal phase.

Mitzi et al. reported the intercalation of perfluoro-aryl within the layer of aryl cations in tin iodide-based perovskites[26] and bimolecular perovskites using pentafluorophenethylammonium and naphthyleneethylammonium cations.[27] This advance highlighted the importance of the noncovalent fluoroaryl−aryl interaction in constructing intercalated organic perovskites. Researchers then reported the intercalation in perovskites by donor−acceptor charge transfer complexes,[28,29] molecular iodide,[30] and tetrachloro-1,2-benzoquinone.[31] However, our understanding of effective intermolecular interactions in perovskites is still insufficient for the design of polar bimolecular systems. The interactions studied so far have mostly involved symmetric (nonpolar) organic modules with limited chemical and functional versatility for organic design.

In our search for effective interactions of organic pairs within the perovskite framework, we explored a broad range of polar functional groups. We chose Pb-based perovskites over other metals (e.g., Sn and Ge) because of their stability and robustness. Our study honed in on thin film crystallization, a process easily integrated into waveguide electro-optic modulators.

We used two classes of molecules: primary cationic and secondary neutral molecules. Primary organics are ammonium cations with hydroxyl, methoxy, halogen, and ether functional groups in either aliphatic or aromatic backbones (Figure 1E). Secondary organics are neutral molecules that contain halogen, methoxy, amine, nitro, and cyan functional groups (Figure 1F). The aromatic molecules selected here possess a high dipole

Received: October 31, 2023
Revised: December 1, 2023
Accepted: December 4, 2023
Published: December 7, 2023

https://doi.org/10.1021/jacs.3c12172
J. Am. Chem. Soc. 2023, 145, 27242−27247

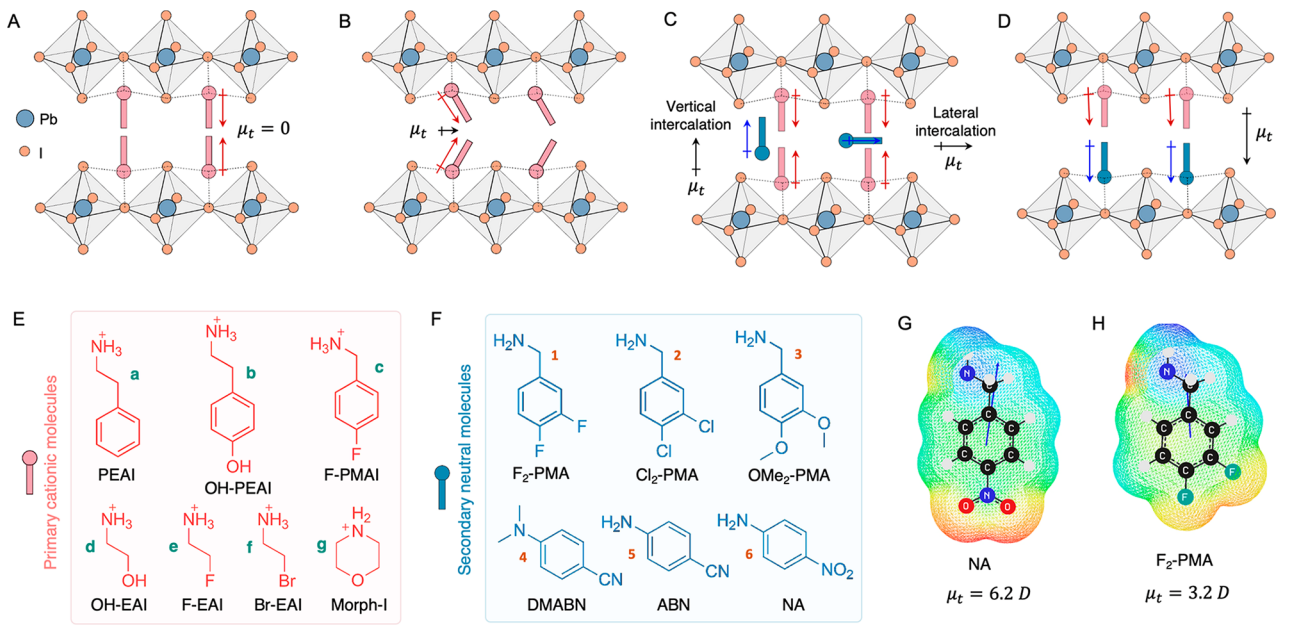

Figure 1. Bimolecular organic perovskite design and molecular modules. Schematics of the mono-organic perovskite scenarios when the organic dipoles are (a) fully canceled and (b) partially canceled. Organic binary perovskites scenario when (c) the secondary organics have been laterally or vertically intercalated and (d) the secondary organics have served as cationic sites (A site). Tested organics: (e) primary organics (primary cationic molecules) and (f) secondary organics (secondary neutral molecules). Charge mapping density and calculated dipoles for (g) 4-nitroaniline (NA) and (h) 3,4-fluoro-phenylmethylammonium (F_2−PMA). μ_t stands for total dipole moment and is calculated using density functional theory (DFT).

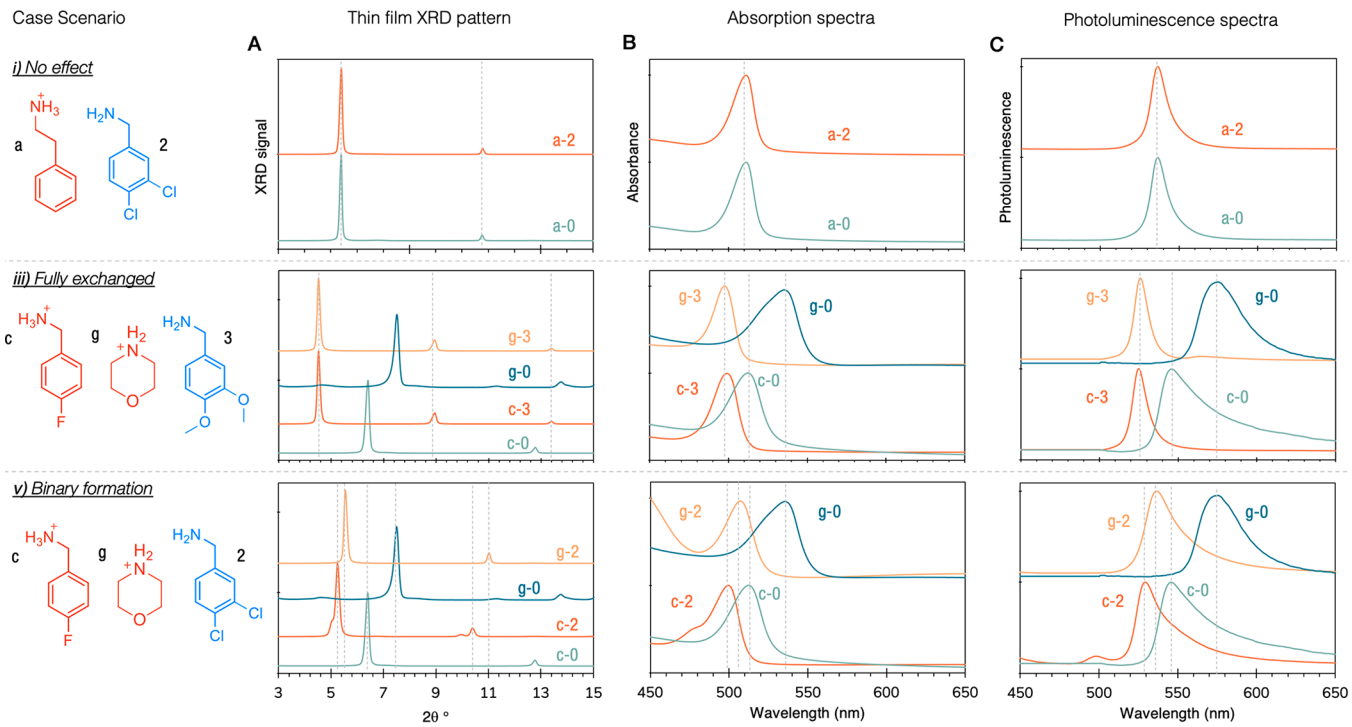

Figure 2. Perovskite crystallization scenarios for organic mixed pairs. (a) Thin film XRD pattern, (b) absorption spectra, and (c) photoluminescence spectra for three examples of different scenarios: (i) "no effect" case for the a-2 organic pair Cl_2−PMA because secondary molecules do not incorporate into perovskites and have no effect on the original phase of the perovskites with primary molecule; (ii) fully exchanged case for the c-3 and g-3 pairs where OMe_2−PMA will accept the proton from the primary molecules and crystallize into the perovskites as mono-organic in which case the primary molecule, itself, becomes irrelevant; and (iii) bimolecular formation case for the c-2 and g-2 pairs where both organic pairs exist collaboratively within the perovskite's framework. All characterization is of thin films with a secondary to primary organic ratio of 1 and an annealing temperature of 85 °C for 10 min. See Figures S1−S7 for the XRD patterns of all tested pairs.

moment (>2.5 D) and provide chemical functional groups for intermolecular bonding (Figure 1G,H). When they are incorporated, these polar molecules offer added degrees of freedom to engineer polarizability within the perovskite framework, thereby contributing both to nonlinear optics and electro-optic modulation. While the Goldschmidt

https://doi.org/10.1021/jacs.3c12172
J. Am. Chem. Soc. 2023, 145, 27242−27247

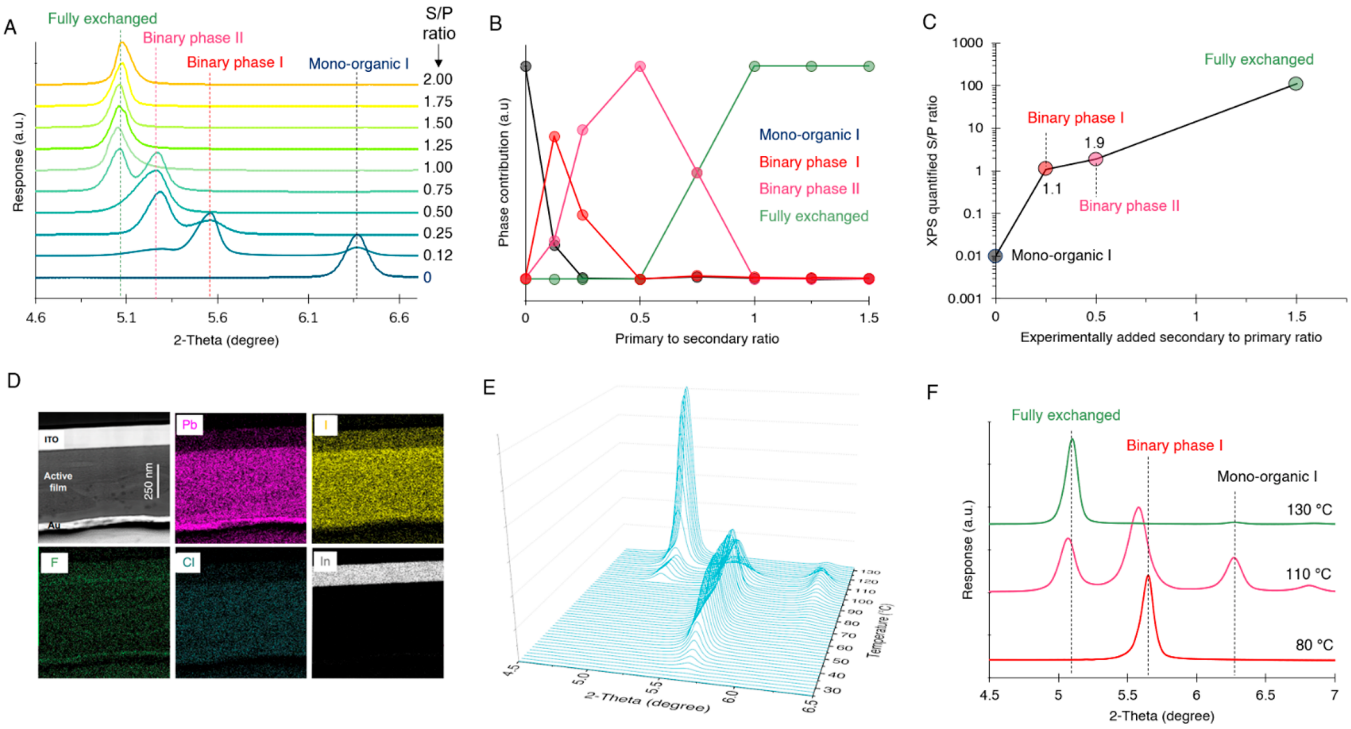

Figure 3. Factors contributing to bimolecular perovskite crystallization scenarios. (a) Overlay of thin film XRD pattern for c-2 pairs with different ratios of Cl_2−PMA (secondary) to F−PMA (primary). The annealing temperature was 85 °C for all samples. (b) The phase diagram of the perovskites with respect to the added ratio of secondary to primary organics. (c) Experimentally determined organic ratio by XPS analysis using Cl and F elements as identifiers for Cl_2−PMA (secondary) and F−PMA (primary) molecules. (d) Elemental mapping across the thin film of c-2 mixture using STEM-EDX (e) in situ thin film XRD pattern analysis for c-2 pair at elevated annealing temperatures. The S/P ratio was constant at 2.0. See Figure S9 for the HR-TEM images and prepared TEM lamella. (f) Overlay of selected XRD pattern from (e) at indicated temperatures.

principles establish the geometrical boundaries for perovskite formability, they are not directly transferable to the intercalation of secondary molecules into the lattice. We discuss spatial considerations for bimolecular perovskites in Supplementary Note 1.

Any intercalation of secondary molecules into the perovskite structure will be evident in the unit cell dimensions. Therefore, we utilized thin film XRD pattern analysis as an initial method of surveying different pairs of primary and secondary molecules (Figures S1−S7). We distinguished five crystallization scenarios upon mixing the organics (see Supplementary Note 2 for the schematics of each scenario):

(i) Secondary molecules do not affect perovskites' original phases (mono-organic). Figure 2i illustrates an example of this scenario. When phenethylammonium iodide (PEAI) (identified by the letter "a") is mixed with Cl_2PMA (identified by the number "2"), it is referred to as the a-2 pair. The index of 0 refers to the original mono-organic perovskites with no addition of secondary molecules (e.g., a-0 in Figure S1). Thin film XRD, absorption, and photoluminescence (PL) profiles of the a-1 mixture remain intact compared with the original mono-organics (a-0). The crystallinity of most mono-organic pairs improves in this scenario, as evidenced by the increased XRD peak intensities. Secondary molecules function as adducts, which slows down the crystallization process, and enhance the quality of resultant thin films (see Figure S8 as an example).

(ii) Secondary molecules hinder the perovskite crystallization process. This can be attributed to the strong interaction between the ammonium tail of the primary molecules and the functional group of the secondary molecules, which suppresses or significantly slows down perovskite film formation (e.g., "a-4" in Figure S1).

(iii) Primary molecules fully transfer their protons to the added secondary molecules. In this case, mono-organic perovskites crystallize with an ammonium version of the secondary molecule as a cation. An example of this scenario is shown in Figure 2iii when F−PMAI ("c") and Morph-I ("g") are mixed with OMe_2PMA ("3"). Although mixed c-3 and g-3 pairs do not share the same primary molecule (cationic site), their XRD pattern, absorption, and PL spectra are identical. This behavior indicates the full proton exchange of F−PMAI or Morph-I with OMe_2−PMA in mono-organic perovskite structures.

(iv) In a less frequent situation when the original mono-organic perovskites exhibit a mixture of different phases, the addition of the secondary molecule selectively renders one of the phases of the original perovskites more prominent (e.g., "b-4"). In this case, although the secondary molecules are not incorporated into the perovskite structure, their interaction with primary cations affects the dominant crystal phase. The choice of secondary molecules results in varying phase distributions, as can be observed when contrasting "b-4" with "b-6" (Figure S2).

(v) The addition of secondary molecules results in the formation of new crystal phases that cannot be explained by the other defined scenarios. In all cases, the interlayer spacing increases compared with the original mono-organic perovskites, which is consistent with the

https://doi.org/10.1021/jacs.3c12172
J. Am. Chem. Soc. 2023, 145, 27242−27247

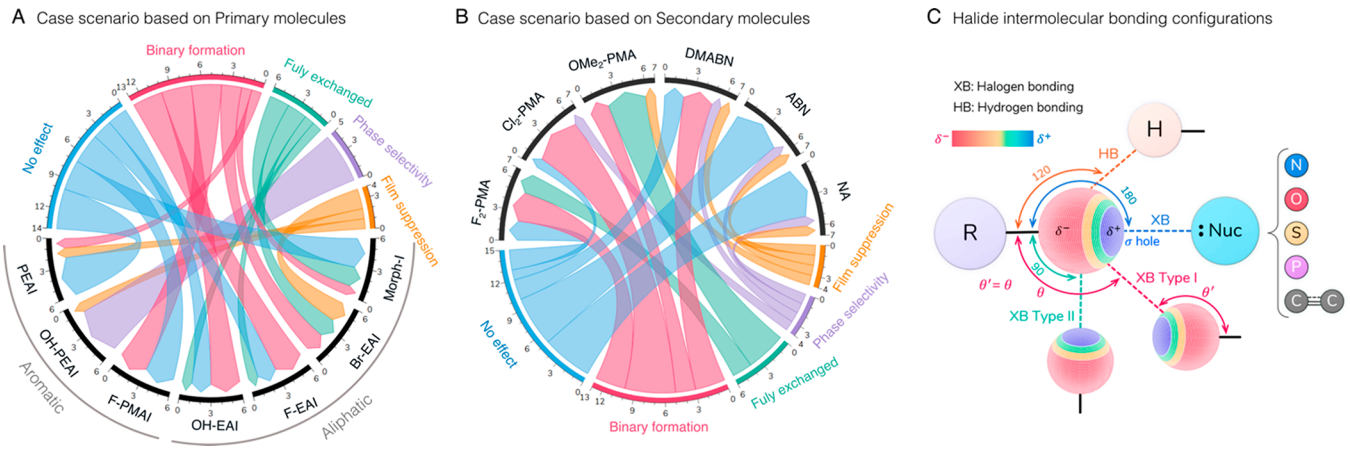

Figure 4. The importance of intermolecular bonding in bimolecular perovskite crystallization. Chord diagrams visualizing the distribution of crystallization scenarios on the basis of the used molecules: (a) primary cationic molecules and (b) secondary neutral molecules. To interpret the diagram, select a specific case scenario from the outer circle and follow its chords to determine its association with either primary or secondary molecule choices. The width of the chord at its base represents the strength of the relationship; a wider base indicates a higher frequency of occurrence. See Table S1 for a tabular presentation of case scenarios based on the tested pair molecules. (c) Schematics of the hydrogen and halogen interaction geometry.

bimolecular formation hypothesis (see Supplementary Note 2). Figure 2v shows an example where F−PMAI ("c") and Morph-I ("g") as primary molecules are mixed with Cl_2PMA ("2") as a secondary molecule. c-2 and g-2 pairs display shifted XRD patterns, absorption, and PL spectra, which differ from all other mixture pairs. These binary systems show a blue shift in absorption and PL peak positions as the interlayer spacing increases (see Supplementary Note 3).

We investigated how the secondary-to-primary entity ratio (S/P) affects the thin film phase. As shown in Figure 3A, increasing the S/P ratio from 0 to 2.0 for the c-2 pair mixture leads to the evolution of the crystal phase from the original mono-organic to fully exchanged secondary mono-organic perovskites. The first binary phase arises when the primary organic cation is eight times more concentrated than the secondary organic molecules. The second binary phase dominates by increasing the concentration of secondary molecules to reach an S/P ratio of 0.5. Notably, binary phase II exhibits a wider interlayer spacing compared with binary phase I (see Figure 3B).

In order to verify if the phases identified by XRD correspond to the organic binary, we employed X-ray photoemission spectroscopy (XPS) to quantify the distinctive elements from primary and secondary molecules present in the perovskite thin film. The c-2 pair mixture was selected, and we used F-to-Cl elemental ratio to determine the S/P molecular ratio. In agreement with thin film XRD studies, the results confirmed the formation of binary perovskites when the secondary and primary molecules were added with an S/P ratio of ∼0.5−1.0, which corresponds to the determined S/P ratio of ∼1−2 by XPS. The system evolved into full exchange when the ratio surpassed 1.0. Scanning transmission electron microscopy−energy dispersive X-ray (STEM-EDS) analysis was conducted to examine the distribution of these elements across their thin film cross-section and determine if agglomeration occurred at the interfaces. The results indicate a uniform distribution of primary and secondary molecules in the resultant films, albeit with different quantities depending on the experimentally added ratio (Figure 3D).

We have extended our investigation into the dynamics of binary phase formation by maintaining a fixed secondary-to-primary molecule ratio of 2.0 and conducting in situ monitoring of the XRD pattern during annealing at elevated temperatures, as presented in Figure 3E,F. In the case of the c-2 pair mixture that has been spin-coated, binary crystals remain the dominant phase up to 80 °C. Peaks corresponding to the original mono-organic and full-exchange scenarios start to emerge at temperatures beyond 90 °C. Ultimately, the full-exchange scenario gains predominance at temperatures exceeding 120 °C. These observations suggest that the final perovskite product is a result of the interplay between thermodynamic and kinetic factors, with temperature playing a significant role in this equation. Elevated temperatures facilitate proton transfer between the primary cationic and secondary neutral molecules, thereby promoting the dominance of the full-exchange scenario. The formation of binary perovskites is sensitive to factors such as the substrate surface, annealing temperature, type of antisolvents, and the ratio of added molecules. This multitude of factors renders the growth of pure and stable single crystals from these binary phases an experimentally challenging task, as elaborated in Supplementary Note 4.

Distinguishing between the binary scenarios hypothesized in Figure 1 panels C and D is challenging without single-crystal XRD (SC-XRD). However, identifying effective intermolecular interactions provides us with a tool for the further design of binary perovskites. Chord diagrams shown in Figure 4A,B visualize the relationship between the identified mixture scenarios and used primary (panel A) and secondary molecules (panel B). The majority of pairs that result in bimolecular formation involve at least one molecule with halogen atoms (F or Cl). Particularly, Cl_2−PMA, when used as a secondary molecule, led to the formation of binary perovskites in approximately 70% of the tested mixtures involving various primary molecules. This stands in contrast to ABN (Aminobenzonitrile) and NA (Nitroaniline), which did not yield binary perovskites in any of their tested mixtures (Table S1). Halogen groups facilitate strong noncovalent interactions, including halogen and hydrogen bonding, which are widely

https://doi.org/10.1021/jacs.3c12172
J. Am. Chem. Soc. 2023, 145, 27242−27247

used in supramolecular and cocrystal engineering.[32−36] Their anisotropic electron density distribution enables interaction with nucleophiles and electrophiles, with interaction type and energy tunable by the halogen atom choice.[6,32,33]

Fluoride atoms engage in hydrogen bonding (HB), while other halogens (I > Br > Cl) favor halogen bonding.[6,32,33] Figure 4C shows nucleophiles interacting with a halogen atom's positively charged sigma hole. Also, halogens can interact with one another in various geometries, classified as Type I and Type II bonding.

We also note the strong propensity of OMe_2−PMA to engage in proton transfer with the primary molecules. This process led to the displacement of the primary molecules from the perovskite structure, thereby resulting in the formation of highly crystalline films comprising solely OMe_2−PMA. Such favorable kinetics and thermodynamics in perovskite crystallization suggest that molecules with methoxy functional groups may serve as desirable organic cations in applications where high stability and crystallinity are critical.

Perovskites with bimolecular organic modules offer flexibility for customized applications. Understanding the effective interactions between organic pairs is crucial for stable binary systems. Halogen bonding (XB) is emerging as a tool to assist in the development of next-generation materials, and recent studies have linked XB to improved perovskite photovoltaic performance.[6,34,35,37−39] On the basis of our thin film analysis across 42 distinct mixture scenarios—a format readily compatible with integration into waveguide platforms—we underscore the significant potential of XB and HB interactions in the design of organic modules for bimolecular hybrid perovskites. Insights gained from this study are further applicable to the engineering of structures specifically tailored for advanced functionalities, including chemical storage,[40] spintronics, and nonlinear optics. To achieve structural resolution of these bimolecular stacked structures, additional investigations focused on the synthesis of pure binary phase single crystals are needed.

■ ASSOCIATED CONTENT

Supporting Information

The Supporting Information is available free of charge at https://pubs.acs.org/doi/10.1021/jacs.3c12172.

Experimental procedure details and methods, thin film XRD pattern of the perovskite thin films with tested organics pairs, SEM and HR-TEM images, table of the identified crystallization scenarios upon mixing the organics, and supplementary notes 1−4 (PDF)

XRD data of the fabricated thin films (XLSX)

■ AUTHOR INFORMATION

Corresponding Author

Edward H. Sargent − *Department of Electrical and Computer Engineering, University of Toronto, Toronto M5S 3G4, Canada;* orcid.org/0000-0003-0396-6495; Email: ted.sargent@utoronto.ca

Authors

Amin Morteza Najarian − *Department of Electrical and Computer Engineering, University of Toronto, Toronto M5S 3G4, Canada;* orcid.org/0000-0002-0455-0451

Maral Vafaie − *Department of Electrical and Computer Engineering, University of Toronto, Toronto M5S 3G4, Canada;* orcid.org/0000-0001-9119-6499

Randy Sabatini − *Department of Electrical and Computer Engineering, University of Toronto, Toronto M5S 3G4, Canada;* orcid.org/0000-0002-5975-4347

Sasa Wang − *Department of Electrical and Computer Engineering, University of Toronto, Toronto M5S 3G4, Canada*

Peng Li − *NanoFAB, University of Alberta, Edmonton, Alberta T6G 2V4, Canada*

Shihong Xu − *NanoFAB, University of Alberta, Edmonton, Alberta T6G 2V4, Canada*

Makhsud I. Saidaminov − *Department of Chemistry, University of Victoria, Victoria, British Columbia V8P 5C2, Canada;* orcid.org/0000-0002-3850-666X

Sjoerd Hoogland − *Department of Electrical and Computer Engineering, University of Toronto, Toronto M5S 3G4, Canada;* orcid.org/0000-0002-3099-585X

Complete contact information is available at: https://pubs.acs.org/10.1021/jacs.3c12172

Funding

This work was financially supported by Huawei Technologies Canada Co., Ltd. and the Natural Sciences and Engineering Research Council (NSERC).

Notes

The authors declare no competing financial interest.

■ ACKNOWLEDGMENTS

We acknowledge XPS and TEM services provided by Nanofab at the University of Alberta.

■ REFERENCES

(1) Saparov, B.; Mitzi, D. B. Organic-Inorganic Perovskites: Structural Versatility for Functional Materials Design. *Chem. Rev.* **2016**, *116* (7), 4558−4596.

(2) Blancon, J. C.; Even, J.; Stoumpos, C. C.; Kanatzidis, M. G.; Mohite, A. D. Semiconductor Physics of Organic−Inorganic 2D Halide Perovskites. *Nat. Nanotechnol* **2020**, *15* (12), 969−985.

(3) Leng, K.; Fu, W.; Liu, Y.; Chhowalla, M.; Loh, K. P. From Bulk to Molecularly Thin Hybrid Perovskites. *Nat. Rev. Mater.* **2020**, *5* (7), 482−500.

(4) Song, T.; Ma, Q. X.; Wang, Q.; Zhang, H. L. Design of Two-Dimensional Halide Perovskite Composites for Optoelectronic Applications and Beyond. *Mater. Adv.* **2022**, *3* (2), 756−778.

(5) Katan, C.; Mercier, N.; Even, J. Quantum and Dielectric Confinement Effects in Lower-Dimensional Hybrid Perovskite Semiconductors. *Chem. Rev.* **2019**, *119* (5), 3140−3192.

(6) Morteza Najarian, A.; Dinic, F.; Chen, H.; Sabatini, R.; Zheng, C.; Lough, A.; Maris, T.; Saidaminov, M. I.; García de Arquer, F. P.; Voznyy, O.; Hoogland, S.; Sargent, E. H. Homomeric Chains of Intermolecular Bonds Scaffold Octahedral Germanium Perovskites. *Nature* **2023**, *620* (7973), 328−335.

(7) Smith, M. D.; Connor, B. A.; Karunadasa, H. I. Tuning the Luminescence of Layered Halide Perovskites. *Chem. Rev.* **2019**, *119* (5), 3104−3139.

(8) Zhang, L.; Sun, C.; He, T.; Jiang, Y.; Wei, J.; Huang, Y.; Yuan, M. High-Performance Quasi-2D Perovskite Light-Emitting Diodes: From Materials to Devices. *Light Sci. Appl.* **2021**, *10* (1), 1−26.

(9) Wang, N.; Cheng, L.; Ge, R.; Zhang, S.; Miao, Y.; Zou, W.; Yi, C.; Sun, Y.; Cao, Y.; Yang, R.; Wei, Y.; Guo, Q.; Ke, Y.; Yu, M.; Jin, Y.; Liu, Y.; Ding, Q.; Di, D.; Yang, L.; Xing, G.; Tian, H.; Jin, C.; Gao, F.; Friend, R. H.; Wang, J.; Huang, W. Perovskite Light-Emitting Diodes

Based on Solution-Processed Self-Organized Multiple Quantum Wells. *Nat. Photonics* **2016**, *10* (11), 699−704.
(10) Shen, D.; Ren, Z.; Li, Q.; Luo, C.; Xia, W.; Zheng, Z.; Ma, W.; Li, J.; Chen, Y. Highly Emissive Quasi-2D Perovskites Enabled by a Multifunctional Molecule for Bright Light-Emitting Diodes. *ACS Appl. Mater. Interfaces* **2022**, *2022*, 21636.
(11) Gong, X.; Voznyy, O.; Jain, A.; Liu, W.; Sabatini, R.; Piontkowski, Z.; Walters, G.; Bappi, G.; Nokhrin, S.; Bushuyev, O.; Yuan, M.; Comin, R.; McCamant, D.; Kelley, S. O.; Sargent, E. H. Electron-Phonon Interaction in Efficient Perovskite Blue Emitters. *Nat. Mater.* **2018**, *17* (6), 550−556.
(12) Hu, T.; Smith, M. D.; Dohner, E. R.; Sher, M. J.; Wu, X.; Trinh, M. T.; Fisher, A.; Corbett, J.; Zhu, X. Y.; Karunadasa, H. I.; Lindenberg, A. M. Mechanism for Broadband White-Light Emission from Two-Dimensional (110) Hybrid Perovskites. *J. Phys. Chem. Lett.* **2016**, *7* (12), 2258−2263.
(13) Jana, M. K.; Song, R.; Xie, Y.; Zhao, R.; Sercel, P. C.; Blum, V.; Mitzi, D. B. Structural Descriptor for Enhanced Spin-Splitting in 2D Hybrid Perovskites. *Nat. Commun.* **2021**, *12* (1), 1−10.
(14) Wei, W. J.; Jiang, X. X.; Dong, L. Y.; Liu, W. W.; Han, X. B.; Qin, Y.; Li, K.; Li, W.; Lin, Z. S.; Bu, X. H.; Lu, P. X. Regulating Second-Harmonic Generation by van Der Waals Interactions in Two-Dimensional Lead Halide Perovskite Nanosheets. *J. Am. Chem. Soc.* **2019**, *141* (23), 9134−9139.
(15) Yuan, C.; Li, X.; Semin, S.; Feng, Y.; Rasing, T.; Xu, J. Chiral Lead Halide Perovskite Nanowires for Second-Order Nonlinear Optics. *Nano Lett.* **2018**, *18* (9), 5411−5417.
(16) Ahn, J.; Lee, E.; Tan, J.; Yang, W.; Kim, B.; Moon, J. A New Class of Chiral Semiconductors: Chiral-Organic-Molecule-Incorporating Organic-Inorganic Hybrid Perovskites. *Mater. Horiz* **2017**, *4* (5), 851−856.
(17) Lin, J. T.; Chen, D. G.; Yang, L. S.; Lin, T. C.; Liu, Y. H.; Chao, Y. C.; Chou, P. T.; Chiu, C. W. Tuning the Circular Dichroism and Circular Polarized Luminescence Intensities of Chiral 2D Hybrid Organic−Inorganic Perovskites through Halogenation of the Organic Ions. *Angewandte Chemie - International Edition* **2021**, *60* (39), 21434−21440.
(18) Yang, C. K.; Chen, W. N.; Ding, Y. T.; Wang, J.; Rao, Y.; Liao, W. Q.; Tang, Y. Y.; Li, P. F.; Wang, Z. X.; Xiong, R. G. The First 2D Homochiral Lead Iodide Perovskite Ferroelectrics: [R- and S-1-(4-Chlorophenyl)Ethylammonium] 2 PbI 4. *Adv. Mater.* **2019**, *31* (16), No. 1808088.
(19) Wang, S.; Liu, X.; Li, L.; Ji, C.; Sun, Z.; Wu, Z.; Hong, M.; Luo, J. An Unprecedented Biaxial Trilayered Hybrid Perovskite Ferroelectric with Directionally Tunable Photovoltaic Effects. *J. Am. Chem. Soc.* **2019**, *141* (19), 7693−7697.
(20) Li, L.; Sun, Z.; Wang, P.; Hu, W.; Wang, S.; Ji, C.; Hong, M.; Luo, J. Tailored Engineering of an Unusual $(C_4H_9NH_3)_2(CH_3NH_3)_2Pb_3Br_{10}$ Two-Dimensional Multilayered Perovskite Ferroelectric for a High-Performance Photodetector. *Angew. Chem.* **2017**, *129* (40), 12318−12322.
(21) Ma, J.; Fang, C.; Chen, C.; Jin, L.; Wang, J.; Wang, S.; Tang, J.; Li, D. Chiral 2D Perovskites with a High Degree of Circularly Polarized Photoluminescence. *ACS Nano* **2019**, *13* (3), 3659−3665.
(22) Trujillo-Hernández, K.; Rodríguez-López, G.; Espinosa-Roa, A.; González-Roque, J.; Gómora-Figueroa, A. P.; Zhang, W.; Halasyamani, P. S.; Jancik, V.; Gembicky, M.; Pirruccio, G.; Solis-Ibarra, D. Chirality Control in White-Light Emitting 2D Perovskites. *J. Mater. Chem. C Mater.* **2020**, *8* (28), 9602−9607.
(23) Ma, S.; Jung, Y. K.; Ahn, J.; Kyhm, J.; Tan, J.; Lee, H.; Jang, G.; Lee, C. U.; Walsh, A.; Moon, J. Elucidating the Origin of Chiroptical Activity in Chiral 2D Perovskites through Nano-Confined Growth. *Nat. Commun.* **2022**, *13* (1), 1−10.
(24) Gao, Y.; Sachinthani, K. A. N.; Zheng, C.; Jarrett-Wilkins, C.; Johnston, A.; Sun, M. J.; Najarian, A. M.; Wang, Y. K.; Saidaminov, M. I.; de Arquer, F. P. G.; Seferos, D. S.; Hoogland, S.; Sargent, E. H. Self-Aligned Non-Centrosymmetric Conjugated Molecules Enable Electro-Optic Perovskites. *Adv. Opt Mater.* **2021**, *9* (20), No. 2100730.
(25) Gao, Y.; Walters, G.; Qin, Y.; Chen, B.; Min, Y.; Seifitokaldani, A.; Sun, B.; Todorovic, P.; Saidaminov, M. I.; Lough, A.; Tongay, S.; Hoogland, S.; Sargent, E. H. Electro-Optic Modulation in Hybrid Metal Halide Perovskites. *Adv. Mater.* **2019**, *31* (16), No. 1808336.
(26) Mitzi, D. B.; Medeiros, D. R.; Malenfant, P. R. L. Intercalated Organic-Inorganic Perovskites Stabilized by Fluoroaryl-Aryl Interactions. *Inorg. Chem.* **2002**, *41* (8), 2134−2145.
(27) Xu, Z.; Mitzi, D. B. SnI42–Based Hybrid Perovskites Templated by Multiple Organic Cations: Combining Organic Functionalities through Noncovalent Interactions. *Chem. Mater.* **2003**, *15* (19), 3632−3637.
(28) Van Gompel, W. T. M.; Herckens, R.; Van Hecke, K.; Ruttens, B.; D'Haen, J.; Lutsen, L.; Vanderzande, D. Towards 2D Layered Hybrid Perovskites with Enhanced Functionality: Introducing Charge-Transfer Complexes: Via Self-Assembly. *Chem. Commun.* **2019**, *55* (17), 2481−2484.
(29) Marchal, N.; Van Gompel, W.; Gélvez-Rueda, M. C.; Vandewal, K.; Van Hecke, K.; Boyen, H. G.; Conings, B.; Herckens, R.; Maheshwari, S.; Lutsen, L.; Quarti, C.; Grozema, F. C.; Vanderzande, D.; Beljonne, D. Lead-Halide Perovskites Meet Donor-Acceptor Charge-Transfer Complexes. *Chem. Mater.* **2019**, *31* (17), 6880−6888.
(30) Smith, M. D.; Pedesseau, L.; Kepenekian, M.; Smith, I. C.; Katan, C.; Even, J.; Karunadasa, H. I. Decreasing the Electronic Confinement in Layered Perovskites through Intercalation. *Chem. Sci.* **2017**, *8* (3), 1960−1968.
(31) Passarelli, J. V.; Mauck, C. M.; Winslow, S. W.; Perkinson, C. F.; Bard, J. C.; Sai, H.; Williams, K. W.; Narayanan, A.; Fairfield, D. J.; Hendricks, M. P.; Tisdale, W. A.; Stupp, S. I. Tunable Exciton Binding Energy in 2D Hybrid Layered Perovskites through Donor−Acceptor Interactions within the Organic Layer. *Nat. Chem.* **2020**, *12* (8), 672−682.
(32) Kellett, C. W.; Kennepohl, P.; Berlinguette, C. P. π Covalency in the Halogen Bond. *Nat. Commun.* **2020**, *11* (1), 3310.
(33) Cavallo, G.; Metrangolo, P.; Milani, R.; Pilati, T.; Priimagi, A.; Resnati, G.; Terraneo, G. The Halogen Bond. *Chem. Rev.* **2016**, *116* (4), 2478−2601.
(34) Metrangolo, P.; Canil, L.; Abate, A.; Terraneo, G.; Cavallo, G. Halogen Bonding in Perovskite Solar Cells: A New Tool for Improving Solar Energy Conversion. *Angewandte Chemie - International Edition* **2022**, *61* (11), No. e202114793.
(35) Ball, M. L.; Milic, J. V.; Loo, Y. L. The Emerging Role of Halogen Bonding in Hybrid Perovskite Photovoltaics. *Chem. Mater.* **2022**, *34*, 2495.
(36) Varadwaj, P. R.; Varadwaj, A.; Marques, H. M. Halogen Bonding: A Halogen-Centered Noncovalent Interaction yet to Be Understood. *Inorganics (Basel)* **2019**, *7* (3), 40.
(37) Canil, L.; Cramer, T.; Fraboni, B.; Ricciarelli, D.; Meggiolaro, D.; Singh, A.; Liu, M.; Rusu, M.; Wolff, C. M.; Phung, N.; Wang, Q.; Neher, D.; Unold, T.; Vivo, P.; Gagliardi, A.; De Angelis, F.; Abate, A. Tuning Halide Perovskite Energy Levels. *Energy Environ. Sci.* **2021**, *14* (3), 1429−1438.
(38) Ruiz-Preciado, M. A.; Kubicki, D. J.; Hofstetter, A.; McGovern, L.; Futscher, M. H.; Ummadisingu, A.; Gershoni-Poranne, R.; Zakeeruddin, S. M.; Ehrler, B.; Emsley, L.; Milić, J. V.; Grätzel, M. Supramolecular Modulation of Hybrid Perovskite Solar Cells via Bifunctional Halogen Bonding Revealed by Two-Dimensional 19F Solid-State NMR Spectroscopy. *J. Am. Chem. Soc.* **2020**, *142* (3), 1645−1654.
(39) Bi, S.; Wang, H.; Zhou, J.; You, S.; Zhang, Y.; Shi, X.; Tang, Z.; Zhou, H. Halogen Bonding Reduces Intrinsic Traps and Enhances Charge Mobilities in Halide Perovskite Solar Cells. *J. Mater. Chem. A Mater.* **2019**, *7* (12), 6840−6848.
(40) Rajappa Muralidhar, J.; Salikolimi, K.; Adachi, K.; Hashizume, D.; Kodama, K.; Hirose, T.; Ito, Y.; Kawamoto, M. Chemical Storage of Ammonia through Dynamic Structural Transformation of a Hybrid Perovskite Compound. *J. Am. Chem. Soc.* **2023**, *145*, 16973.

https://doi.org/10.1021/jacs.3c12172
J. Am. Chem. Soc. 2023, 145, 27242−27247